Resolving the VO_2 controversy: Mott mechanism dominates the insulator-to-metal transition

O. Nájera,[1] M. Civelli,[1] V. Dobrosavljević,[2] and M. J. Rozenberg[1]
[1]*Laboratoire de Physique des Solides, CNRS-UMR8502, Université Paris-Sud, Orsay 91405, France*
[2]*Department of Physics and National High Magnetic Field Laboratory, Florida State University, Tallahassee, Florida 32306, USA*
(Received 3 June 2016; published 9 January 2017)

We consider a minimal model to investigate the metal-insulator transition in VO_2. We adopt a Hubbard model with two orbitals per unit cell, which captures the competition between Mott and singlet-dimer localization. We solve the model within dynamical mean-field theory, characterizing in detail the metal-insulator transition and finding new features in the electronic states. We compare our results with available experimental data, obtaining good agreement in the relevant model parameter range. Crucially, we can account for puzzling optical conductivity data obtained within the hysteresis region, which we associate with a metallic state characterized by a split heavy quasiparticle band. Our results show that the thermal-driven insulator-to-metal transition in VO_2 is compatible with a Mott electronic mechanism, providing fresh insight to a long-standing "chicken-and-egg" debate and calling for further research of "Mottronics" applications of this system.

DOI: 10.1103/PhysRevB.95.035113

Vanadium dioxide VO_2 and vanadium sesquioxide V_2O_3 remain at the center stage of condensed-matter physics as they are prototypical examples of systems undergoing a strongly correlated metal-insulator transition (MIT) [1]. Their unusual electronic behavior makes them very attractive materials for novel electronic devices [2,3]. In fact, they are being investigated intensively in the emerging field of "Mottronics," which aims to exploit the functionalities associated with quantum Mott transitions. A key goal is to create fast and ultralow-power consumption transistors, which may be downsized to the atomic limit [4–6].

VO_2 and V_2O_3 have nominally partially filled bands, hence they are expected to be metals. However, they undergo a first-order metal-to-insulator transition upon cooling at ∼340 and 180 K, respectively. This phenomenon has often been associated with a Mott MIT [1], namely a transition driven by the competition between kinetic energy and Coulomb repulsion [7]. However, that point of view has been questioned just as often [1,8].

The case of VO_2, displaying a transition from a high-T rutile (R) metal to a low-T monoclinic (M_1) insulator is emblematic [9–16]. The central issue is whether the transition is driven by a spin-Peierls structural instability, or by a Mott-Hubbard-type electronic charge localization. This issue has been under scrutiny using electronic structure calculations [17–21] based on the combination of density-functional theory in the local-density approximation with dynamical mean-field theory (LDA+DMFT) [22]. In the pioneering work of Ref. [17], Biermann *et al.* argued that the insulator should be considered as a renormalized Peierls insulator, i.e., a band-insulator where the opening of the bonding-antibonding gap is driven by dimerization and renormalized down by interactions [17]. On the other hand, the calculations showed that within the metallic rutile phase, the Coulomb interaction failed to produce a MIT for reasonable values of the interaction. More recently, the problem was reconsidered by Brito *et al.* [19] and by Biermann *et al.* as well [20,23–25], providing a rather different scenario. Brito *et al.* found a MIT within a second monoclinic (M_2) phase of VO_2 that only has half the dimerization of the standard M_1 for the same value of the Coulomb interaction. Hence, they argued that Mott localization must play the leading role in both MITs. Nevertheless, they also noted that the Mott insulator adiabatically connects to the singlet dimer insulator state, and therefore the transition should be considered a Mott-Hubbard transition in the presence of strong intersite exchange [19,20,23].

While those LDA+DMFT works provided multiple useful insights, the issue of whether the first-order MIT at 340 K in VO_2 is electronically or structurally driven still remains. Here we shall try to shed new light on this classic "chicken-and-egg" problem by adopting a different strategy. We shall trade the complications of the realistic crystal structures and orbital degeneracy of VO_2 for a model Hamiltonian, namely the dimer Hubbard model (DHM), that captures the key competition between Mott localization due to Coulomb repulsion and singlet dimerization, i.e., Peierls localization. This permits a detailed systematic study that may clearly expose the physical mechanisms at play. Importantly, in our study the underlying lattice *stays put*. Therefore, we can directly address the issue of whether a purely electronic transition, having a bearing on the physics of VO_2, exists in this model. The specific questions that we shall address are the following: (i) Does this purely electronic model predict a first-order metal-insulator transition as a function of the temperature *within the relevant parameter region*? (ii) What is the physical nature of the different states? (iii) Can they be related to key available experiments? These issues are relevant, since if this basic model fails to predict an electronic MIT consistent with the one observed in VO_2, then it would be mandatory to include the lattice degrees of freedom. In the present study, we shall provide explicit answers to these questions. We show that the solution of the DHM brings the equivalent physical insight for VO_2 as the single-band Hubbard model for V_2O_3, which is one of the significant achievements of DMFT [26,27].

The dimer Hubbard model is defined as

$$H = \left[-t \sum_{\langle i,j\rangle\alpha\sigma} c^{\dagger}_{i\alpha\sigma} c_{j\alpha\sigma} + t_{\perp} \sum_{i\sigma} c^{\dagger}_{i1\sigma} c_{i2\sigma} + \text{H.c.} \right] + \sum_{i\alpha} U n_{i\alpha\uparrow} n_{i\alpha\downarrow}, \quad (1)$$

where $\langle i,j\rangle$ denotes nearest-neighbor (n.n.) lattice sites, $\alpha = \{1,2\}$ denote the dimer orbitals, σ is the spin, t is the lattice hopping, $t_\perp$ is the intradimer hopping, and U is the Coulomb repulsion. For simplicity, we adopt a semicircular density of states $\rho(\varepsilon) = \sqrt{4t^2 - \varepsilon^2}/(2\pi t^2)$. The energy unit is set by $t = 1/2$, which gives a full bandwidth of $4t = 2D = 2$, where D is the half-bandwidth. This interesting model has received surprisingly little attention, and only partial solutions have been obtained within DMFT [28–31]. The main results were the identification of the region of coexistent solutions at moderate U and small $t_\perp$ at $T = 0$ using the iterated perturbation theory (IPT) approximation [28] and at finite $T = 0.025$ by quantum Monte Carlo [32,33] (QMC) [29]. Here we obtain a detailed solution of the problem, paying special attention to the MIT and the nature of the coexistent solutions. We solve for the DMFT equations with hybridization-expansion continuous-time quantum Monte Carlo (CT-QMC) [34,35] and exact diagonalization [26], which provide (numerically) exact solutions. We also adopt the IPT approximation [28], which, remarkably, we find is (numerically) exact in the atomic limit $t = 0$, therefore it provides reliable solutions of comparable quality as in the single-band Hubbard model [26]. Furthermore, IPT is extremely fast and efficient to explore the large parameter space of the model, and it provides accurate solutions on the real frequency axis. An extensive comparison between IPT and the CT-QMC is shown in the Supplemental Material [43]. The DMFT equations provide for the exact solution of the DHM in the limit of large lattice coordination, and they have been derived elsewhere [28]. Here we quote the key self-consistency condition of the associated quantum dimer-impurity model,

$$\mathbf{G}^{-1}(i\omega_n) + \mathbf{\Sigma}(i\omega_n) = \begin{pmatrix} i\omega_n & -t_\perp \\ -t_\perp & i\omega_n \end{pmatrix} - t^2\mathbf{G}(i\omega_n), \qquad (2)$$

where $G_{\alpha,\beta}$ and $\Sigma_{\alpha,\beta}$ (with $\alpha,\beta = 1,2$) are, respectively, the dimer-impurity Green's function and self-energy. At the self-consistent point, these two quantities become the respective local quantities of the *lattice* [26]. An important point to emphasize is that this quantum dimer-impurity problem is *analogous* to that in the above-mentioned LDA+DMFT studies [17,19,20,23]. Therefore, strictly speaking, our methodology is a cluster-DMFT (CDMFT) calculation (cf. the Supplemental Material [43]).

We start by establishing the detailed phase diagram, which we show in Fig. 1. We observe that at low T there is a large coexistent region at moderate U and $t_\perp$ below 0.6 [28]. This region gradually shrinks as T is increased, and fully disappears at $T \approx 0.04$. The lower panel shows the phase diagram in the U-T plane at fixed $t_\perp$. At $t_\perp = 0$ we recover the well-known single-band Hubbard model result, where the coexistent region extends in a triangular region defined by the lines $U_{c1}(T)$ and $U_{c2}(T)$ [26]. The triangle is tilted to the left, which indicates that upon warming the correlated metal undergoes a first-order transition to a finite-T Mott insulator. This behavior was immediately associated with the famous first-order MIT observed in *Cr-doped* V_2O_3 [26,36], which has long been considered a prime example of a Mott-Hubbard transition [1]. It is noteworthy that this physical feature has remained relevant even in recent LDA+DMFT studies, where the full complexity

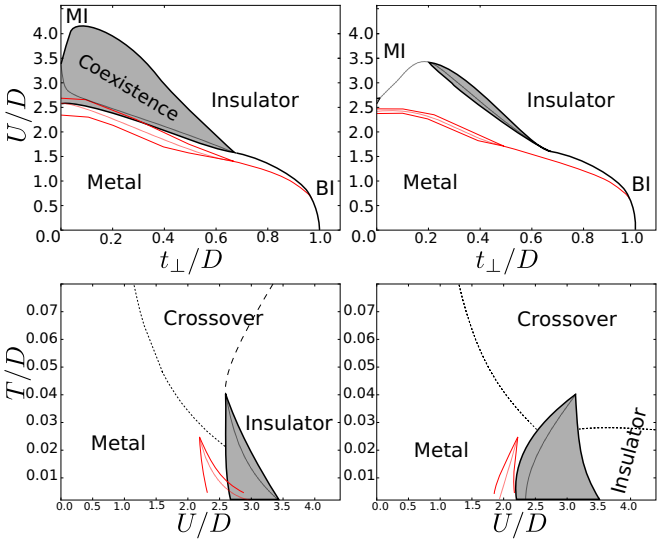

FIG. 1. Phase diagram showing the coexistence (grayed) of metal and insulator states (black lines from IPT and red from QMC), where the approximate position of the first-order lines is indicated. MI denotes Mott insulator and BI denotes bond insulator; the crossover regions have bad metal behavior (see the text and Ref. [40]). The top panels show the $t_\perp$-U plane. The left one shows lower temperature $T = 0.001$ (IPT) and $1/200$ (CT-QMC), and the right one shows higher temperature $T = 0.03$ (IPT) and $1/64$ (CT-QMC). Lower panels show the U-T plane. The left one is for fixed $t_\perp = 0$ (i.e., the single-band Hubbard model), and right one is for $t_\perp = 0.3$.

of the lattice and orbital degeneracy is considered [8,37]. This underlines the utility of sorting the detailed behavior of basic model Hamiltonians. Significantly, as $t_\perp$ is increased in the DHM, the tilt of the triangular region evolves toward the right. This signals that $t_\perp$ fundamentally changes the stability of the ground state. In fact, as shown in the lower right panel of Fig. 1, at $t_\perp = 0.3$ we find that the MIT is *reversed* with respect to the previous case. Namely, upon warming, an insulator undergoes a first-order transition to a (bad) correlated metal at finite T. We may connect several features of this MIT to VO_2, both qualitatively and semiquantitatively. We first consider the energy scales and compare the parameters of the DHM to those of electronic structure calculations. The LDA estimate of the bandwidth of the metallic state of VO_2 is $\sim$2 eV [17], which corresponds in our model to $4t$, hence $t = 0.5$ eV. This is handy, since from our choice of $t = 0.5$ we may simply read the numerical energy values of the figures directly in physical units (eV) and compare with experimental data of VO_2. We notice that the coexistence region (with a first-order transition line) extends up to $T \approx 0.04$ (eV) $\approx$400 K, consistent with the experimental value $\approx$340 K. We then set the value of $t_\perp = 0.3$ eV, which corresponds approximately with LDA estimates for the (average) intradimer hopping amplitudes (cf. the Supplemental Material [43]) [17,38,39]. Thus, the coexistence region is centered around $U \approx 2.5$–3 eV, consistent with the values adopted in the LDA+DMFT studies [17,38].

We can make further interesting connections with experiments in VO_2. The metallic state is unusual and it can be characterized as a *bad metal*, i.e., a metal with an anomalously high scattering rate that approaches (or may violate) the

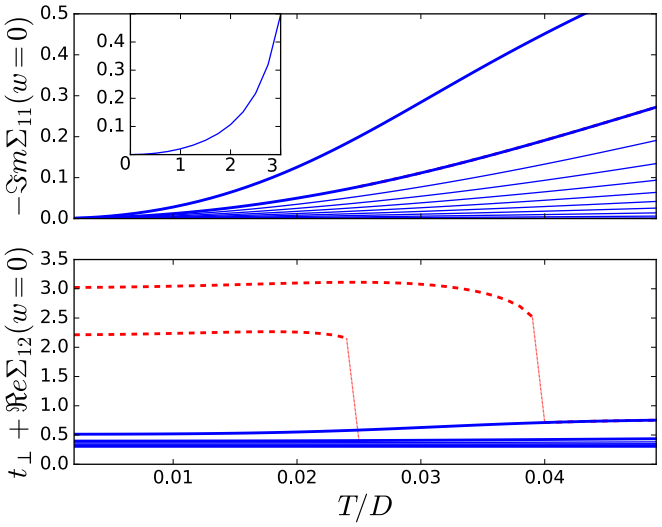

FIG. 2. Top: The scattering rate $\mathrm{Im}[\Sigma_{11}(\omega = 0)]$ for the metal (solid) at fixed $t_\perp = 0.3$ values of U from 0 to 3 in steps of 0.5 (upward). The experimentally relevant values $U = 2.5$ and 3 are highlighted with thick lines. The inset shows the U dependence at fixed $T = 0.04$. Bottom: The effective intradimer hopping $t_\perp^{\mathrm{eff}} = t_\perp + \mathrm{Re}[\Sigma_{12}](0)$ as a function of T for the same parameters as the top panel. Metal states are shown by solid (blue) lines, and the insulator is shown by dashed (red) lines for $U = 2.5$ and 3. The calculations are done with IPT.

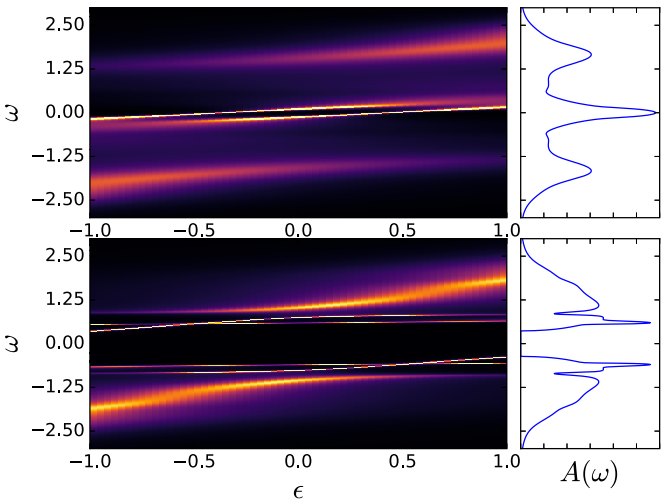

FIG. 3. Electronic dispersion for the metal (left top) and insulator (left bottom) in the coexistence region for parameter values $t_\perp = 0.3$, $U = 2.5$, and $T = 0.01$. Right panels show the respective DOS(ω). The calculations are done with IPT (cf. the Supplemental Material [43]).

Ioffe-Regel limit [41]. In Fig. 2, we show the imaginary part of the diagonal self-energy, whose y-axis intercept indicates the scattering rate (i.e., inverse scattering time). At $T \approx 0.04$ (i.e., ~400 K), we observe a large value of the intercept, of order $\sim t = 1/2$, which signals that the carriers are short-lived quasiparticles. In fact, VO_2 has such an anomalous metallic state [12]. This anomalous scattering is likely the origin of the surprising observation that despite the fact that the lattice structure has one-dimensional (1D) vanadium chains running along the c axis, the resistivity is almost isotropic, within a mere factor of 2 [11]. It is noteworthy that this lack of anisotropy observed in electronic transport experiments provides further justification for our simplified model of a lattice of dimers. This bad metal behavior is a hallmark of Mottness [40,42] and also indicates that the MIT in VO_2 should be characterized as a Mott transition (see Sec. 5 of Ref. [43]). Additional insights on the mechanism driving the transition can be obtained from the behavior of the off-diagonal (intradimer) self-energy $\Sigma_{12}(\omega_n)$. From Eq. (2), we observe that the intradimer hopping amplitude is effectively renormalized as $t_\perp^{\mathrm{eff}} = t_\perp + \mathrm{Re}[\Sigma_{12}](0)$. In Fig. 2, we show the behavior of this quantity across the transition. We see that in the metallic state it remains small, while it becomes large ($\gg t_\perp$) at low T in the insulator [19,20,23]. The physical interpretation is transparent. In the correlated metal, the two dimer sites are primarily Kondo-screened by their lattice neighbors, and as in the single-band Hubbard model, each one forms a heavy quasiparticle band. Then these two bands get split into a bonding and antibonding pair by the small $t_\perp$. Hence, the low-energy electronic structure is qualitatively similar to the noninteracting one, with a larger effective mass. As T is lowered, the dramatic increase in $\mathrm{Re}[\Sigma_{12}](0)$ when the Mott gap opens at the first-order transition signals that the intradimer interaction is boosted by $t_\perp^{\mathrm{eff}} \sim \mathrm{Re}[\Sigma_{12}]$. Unlike the one-band Hubbard model, here the finite $t_\perp$ permits a large energy gain in the Mott insulator by quenching the degenerate entropy. This mechanism, already observed in other cluster-DMFT models [44–46], stabilizes the insulator within the coexistence region, leading to the change in the tilt seen in Fig. 1. Another way of rationalizing the transition is that at a critical U-dependent $t_\perp$, the Kondo screening in the metal breaks down in favor of the local dimer-singlet formation in the insulator. In this view, the large gap opening may be interpreted as a U-driven enhanced band splitting $\propto 2t_\perp^{\mathrm{eff}}(U)$.

Further detail is obtained from a comparison of the electronic structure of the metal and the insulator within the coexistence region. (The electronic structure results from IPT, CT-QMC, and exact diagonalization all show good agreement; see Ref. [43]). In the correlated metallic state shown in Fig. 3, we find at high energies ($\sim \pm U/2$) the incoherent Hubbard bands, which are signatures of Mott physics. At lower energies, we also observe a pair of heavy quasiparticle bands crossing the Fermi energy at $\omega = 0$. Consistent with our previous discussion, this pair of quasiparticle bands can be though of as the renormalization of the noninteracting band structure. Significantly, as we shall discuss later on, this feature may explain the puzzling optical data of Qazilbash *et al.* [12] within the MIT region of VO_2, which has remained unaccounted for so far. Unlike the single-band Hubbard model, the effective mass of these metallic bands does not diverge at the MIT at the critical U, even at $T = 0$. In fact, the finite $t_\perp$ cuts off the effective mass divergence as expected in a model that incorporates spin fluctuations. In addition, the DHM may be considered [28] the simplest nontrivial cluster DMFT model. It is interesting to note that the realistic values $U = 2.5$ and $t_\perp = 0.3$ lead to Hubbard bands at $\approx \pm 1.5$ eV and a quasiparticle residue $Z \approx 0.4$, both consistent with the photoemission experiments of Koethe *et al.* [47].

In Fig. 3, we also show the results for insulator electronic dispersion at the same values of the parameters. The comparison of the insulator and the metal illustrates the significant changes that occur at the first-order MIT. We see that the metallic pair of quasiparticle bands suddenly opens a large gap. More precisely, in contrast to the one-band case, here the Hubbard bands acquire a nontrivial structure, with sharp bands coexisting with incoherent ones. The dispersion of the coherent part can be traced to that of a lattice of singlet dimers (see the Supplemental Material [43]). Hence, the insulator can be characterized as a novel type of Mott-singlet state in which the Hubbard bands have a mixed character with both coherent and incoherent electronic structure contributions. It is also interesting to note that the gap in the density of states is $\Delta \approx 0.6$ eV, again consistent with the photoemission experiments [47].

To gain further insight and make further contact with key experiments, we now consider the optical conductivity response $\sigma(\omega)$ within the MIT coexistence region. A set of remarkable data was obtained in this regime by Qazilbash *et al.* [12], bearing directly on the issue of the driving force behind the transition. They systematically investigated the $\sigma(\omega)$ as a function of T using nanoimaging spectroscopy. They clearly identified within the T range of the MIT the electronic coexistence of insulator and metallic regions, characteristic of a first-order transition. A crucial observation was that upon warming the insulator in the $M1$ phase, metallic puddles emerged with a $\sigma(\omega)$ that was significantly different from the signal of the normal metallic R phase. Thus, the data provided a strong indication of a purely electronic driven transition. Regarding this point, we would like to mention also the works of Arcangeletti *et al.* [15] and Laverock *et al.* [16], who reported the observation of metallic states within the monoclinic phase under pressure and strain, respectively. Coming back to the experiment of Qazilbash *et al.*, a key point that we want to emphasize here is that $\sigma(\omega)$ in the putative $M1$-metallic state was characterized by an intriguing midinfrared (MIR) peak $\omega_{\mathrm{MIR}} \approx 1800\,\mathrm{cm}^{-1} = 0.22$ eV, whose origin was not understood. From our results on the electronic structure within the coexistence region, we find a natural interpretation for the puzzling MIR peak: It corresponds to excitations between the split metallic quasiparticle bands. Since they are parallel, they would produce a significant contribution to $\sigma(\omega)$, which enabled its detection. In Fig. 4, we show the calculated optical conductivity response (see Sec. 7 of the Supplemental Material [43]) that corresponds to the spectra of Fig. 3. In the metal we see that, in fact, a prominent MIR peak is present at $\omega_{\mathrm{MIR}} \approx 0.22$ eV, in excellent agreement with the experimental value. On the other hand, the optical conductivity of the insulator shows a maximum at $\omega_{\mathrm{ins}} \approx 2$ eV in both theory and experiment. Moreover, we also note the good agreement of the relative spectral strengths of the main features in the two phases.

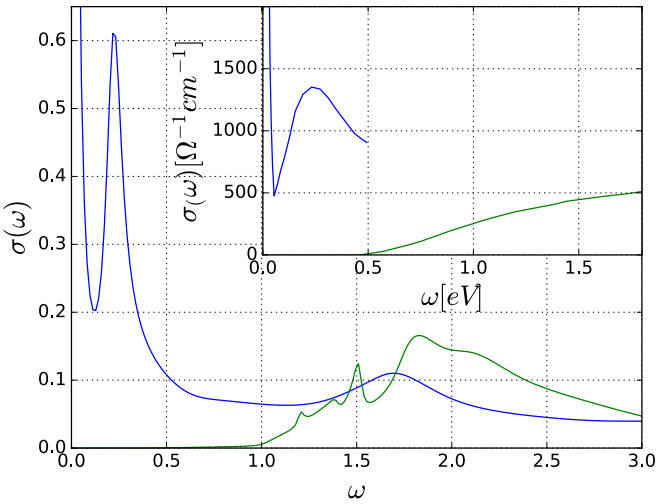

FIG. 4. The optical conductivity $\sigma(\omega)$ of the metal and the insulator within the coexistence region for parameters $t_\perp = 0.3$, $U = 2.5$, and $T = 0.01$. The calculations are done with IPT. Inset: the experimental optical conductivity adapted from Ref. [12].

In conclusion, we showed that the detailed solution of the dimer model treated within DMFT can account for a number of experimental features observed in VO_2. The minimal model has an impurity problem that is analogous to that of LDA+DMFT methods, yet the simplicity of this approach allowed for a detailed solution that permitted a transparent understanding of many physical aspects of the electronic first-order transition in this problem. It exposes a dimer-Mott-transition mechanism, where the effective intradimer exchange is controlled by correlations, weakened in the metal, and strongly enhanced in the Mott insulator. In the metal, this leads to a pair of split quasiparticle bands, which then further separate in the insulator to join and coexist with the usual incoherent Hubbard bands. Despite the simplicity of our model, we made semiquantitative connections to several experimental data in VO_2, including a crucial optical conductivity study within the first-order transition that remained unaccounted for. Our work sheds light on the long-standing question of the driving force behind the metal-insulator transition of VO_2, highlighting the relevance of the Mott mechanism. The present approach may be considered as a counterpart for VO_2 of the DMFT studies of the Mott transition in paramagnetic Cr-doped V_2O_3.

We thank I. Paul, S. Biermann, G. Kotliar, and H.-T. Kim for helpful discussions. This work was partially supported by public grants from the French National Research Agency (ANR), project LACUNES No. ANR-13-BS04-0006-01, and the NSF Grants No. DMR-1005751 and No. DMR-1410132.

[1] M. Imada, A. Fujimori, and Y. Tokura, Metal-insulator transitions, Rev. Mod. Phys. **70**, 1039 (1998).

[2] C. H. Ahn, A. Bhattacharya, M. Di Ventra, J. N. Eckstein, C. Daniel Frisbie, M. E. Gershenson, A. M. Goldman, I. H. Inoue, J. Mannhart, A. J. Millis, A. F. Morpurgo, D. Natelson, and J.-M. Triscone, Electrostatic modification of novel materials, Rev. Mod. Phys. **78**, 1185 (2006).

[3] H. Takagi and H. Y. Hwang, An emergent change of phase for electronics, Science **327**, 1601 (2010).

[4] Z. Yang, C. Ko, and S. Ramanathan, Oxide electronics utilizing ultrafast metal-insulator transitions, Annu. Rev. Mater. Res. **41**, 337 (2011).

[5] M. Nakano, K. Shibuya, D. Okuyama, T. Hatano, S. Ono, M. Kawasaki, Y. Iwasa, and Y. Tokura, Collective bulk carrier delocalization driven by electrostatic surface charge accumulation, Nature (London) **487**, 459 (2012).

[6] J. Jeong, N. Aetukuri, T. Graf, T. D. Schladt, M. G. Samant, and S. S. P. Parkin, Suppression of metal-insulator transition in VO_2 by electric field-induced oxygen vacancy formation, Science (New York, N.Y.) **339**, 1402 (2013).

[7] N. F. Mott, *Metal-Insulator Transitions* (Taylor & Francis, London, 1974).

[8] P. Hansmann, A. Toschi, G. Sangiovanni, T. Saha-Dasgupta, S. Lupi, M. Marsi, and K. Held, Mott-Hubbard transition in V_2O_3 revisited, Phys. Status Solidi B **250**, 1251 (2013).

[9] F. J. Morin, Oxides Which Show a Metal-to-Insulator Transition at the Néel Temperature, Phys. Rev. Lett. **3**, 34 (1959).

[10] J. B. Goodenough, Direct cation-cation interactions in several oxides, Phys. Rev. **117**, 1442 (1960).

[11] P. F. Bongers, Anisotropy of the electrical conductivity of VO_2 single crystals, Solid State Commun. **3**, 275 (1965).

[12] M. M. Qazilbash, M. Brehm, B. G. B.-G. Chae, P.-C. Ho, G. O. Andreev, B.-J. B. J. Kim, S. Y. J. Yun, A. V. Balatsky, M. B. Maple, F. Keilmann, H. T. H.-T. Kim, and D. N. Basov, Mott transition in VO_2 revealed by infrared spectroscopy and nano-imaging, Science **318**, 1750 (2007).

[13] D. Wegkamp, M. Herzog, L. Xian, M. Gatti, P. Cudazzo, C. L. McGahan, R. E. Marvel, R. F. Haglund, A. Rubio, M. Wolf, and J. Stähler, Instantaneous Band Gap Collapse in Photoexcited Monoclinic VO_2 Due to Photocarrier Doping, Phys. Rev. Lett. **113**, 216401 (2014).

[14] N. B. Aetukuri, A. X. Gray, M. Drouard, M. Cossale, L. Gao, A. H. Reid, R. Kukreja, H. Ohldag, C. A. Jenkins, E. Arenholz, K. P. Roche, H. A. Dürr, M. G. Samant, and S. S. P. Parkin, Control of the metal-insulator transition in vanadium dioxide by modifying orbital occupancy, Nat. Phys. **9**, 661 (2013).

[15] E. Arcangeletti, L. Baldassarre, D. Di Castro, S. Lupi, L. Malavasi, C. Marini, A. Perucchi, and P. Postorino, Evidence of a Pressure-Induced Metallization Process in Monoclinic VO_2, Phys. Rev. Lett. **98**, 196406 (2007).

[16] J. Laverock, S. Kittiwatanakul, A. A. Zakharov, Y. R. Niu, B. Chen, S. A. Wolf, J. W. Lu, and K. E. Smith, Direct Observation of Decoupled Structural and Electronic Transitions and an Ambient Pressure Monocliniclike Metallic Phase of VO_2, Phys. Rev. Lett. **113**, 216402 (2014).

[17] S. Biermann, A. Poteryaev, A. I. Lichtenstein, and A. Georges, Dynamical Singlets and Correlation-Assisted Peierls Transition in VO_2, Phys. Rev. Lett. **94**, 026404 (2005).

[18] C. Weber, D. D. O'Regan, N. D. M. Hine, M. C. Payne, G. Kotliar, and P. B. Littlewood, Vanadium Dioxide: A Peierls-Mott Insulator Stable Against Disorder, Phys. Rev. Lett. **108**, 256402 (2012).

[19] W. H. Brito, M. C. O. Aguiar, K. Haule, and G. Kotliar, Metal-Insulator Transition in VO_2 : A DFT + DMFT Perspective, Phys. Rev. Lett. **117**, 056402 (2016).

[20] J. M. Tomczak, F. Aryasetiawan, and S. Biermann, Effective bandstructure in the insulating phase versus strong dynamical correlations in metallic VO_2, Phys. Rev. B **78**, 115103 (2008).

[21] J. M. Tomczak and S. Biermann, Optical properties of correlated materials: Generalized Peierls approach and its application to VO_2, Phys. Rev. B **80**, 085117 (2009).

[22] G. Kotliar, S. Y. Savrasov, K. Haule, V. S. Oudovenko, O. Parcollet, and C. A. Marianetti, Electronic structure calculations with dynamical mean-field theory, Rev. Mod. Phys. **78**, 865 (2006).

[23] J. M. Tomczak and S. Biermann, Effective band structure of correlated materials: The case of VO_2, J. Phys.: Condens. Matter **19**, 365206 (2007).

[24] J. M. Tomczak and S. Biermann, Materials design using correlated oxides: Optical properties of vanadium dioxide, Europhys. Lett. **86**, 37004 (2009).

[25] J. M. Tomczak and S. Biermann, Optical properties of correlated materials—or why intelligent windows may look dirty, Phys. Status Solidi B **246**, 1996 (2009).

[26] A. Georges, G. Kotliar, W. Krauth, and M. Rozenberg, Dynamical mean-field theory of strongly correlated fermion systems and the limit of infinite dimensions, Rev. Mod. Phys. **68**, 13 (1996).

[27] G. Kotliar and D. Vollhardt, Strongly correlated materials: Insights from dynamical mean-field theory, Phys. Today **57**(3), 53 (2004).

[28] G. Moeller, V. Dobrosavljević, and A. E. Ruckenstein, RKKY interactions and the Mott transition, Phys. Rev. B **59**, 6846 (1999).

[29] A. Fuhrmann, D. Heilmann, and H. Monien, From Mott insulator to band insulator: A dynamical mean-field theory study, Phys. Rev. B **73**, 245118 (2006).

[30] H. Hafermann, M. I. Katsnelson, and A. I. Lichtenstein, Metal-insulator transition by suppression of spin fluctuations, Europhys. Lett. **85**, 37006 (2009).

[31] S. S. Kancharla and S. Okamoto, Band insulator to Mott insulator transition in a bilayer Hubbard model, Phys. Rev. B **75**, 193103 (2007).

[32] J. E. Hirsch, Discrete Hubbard-Stratonovich transformation for Fermion lattice models, Phys. Rev. B **28**, 4059 (1983).

[33] J. E. Hirsch and R. M. Fye, Monte Carlo Method for Magnetic Impurities in Metals, Phys. Rev. Lett. **56**, 2521 (1986).

[34] P. Werner and A. J. Millis, Hybridization expansion impurity solver: General formulation and application to Kondo lattice and two-orbital models, Phys. Rev. B **74**, 155107 (2006).

[35] P. Seth, I. Krivenko, M. Ferrero, and O. Parcollet, TRIQS/CTHYB: A continuous-time quantum Monte Carlo hybridisation expansion solver for quantum impurity problems, Comput. Phys. Commun. **200**, 274 (2016).

[36] M. J. Rozenberg, G. Kotliar, and X. Y. Zhang, Mott-Hubbard transition in infinite dimensions. II, Phys. Rev. B **49**, 10181 (1994).

[37] D. Grieger, C. Piefke, O. E. Peil, and F. Lechermann, Approaching finite-temperature phase diagrams of strongly correlated materials: A case study for V_2O_3, Phys. Rev. B **86**, 155121 (2012).

[38] B. Lazarovits, K. Kim, K. Haule, and G. Kotliar, Effects of strain on the electronic structure of VO_2, Phys. Rev. B **81**, 115117 (2010).

[39] A. S. Belozerov, M. A. Korotin, V. I. Anisimov, and A. I. Poteryaev, Monoclinic M_1 phase of VO_2: Mott-Hubbard versus band insulator, Phys. Rev. B **85**, 045109 (2012).

[40] J. Vučičević, D. Tanasković, M. J. Rozenberg, and V. Dobrosavljević, Bad-Metal Behavior Reveals Mott Quantum Criticality in Doped Hubbard Models, Phys. Rev. Lett. **114**, 246402 (2015).

[41] O. Gunnarsson, M. Calandra, and J. E. Han, Colloquium: Saturation of electrical resistivity, Rev. Mod. Phys. **75**, 1085 (2003).

[42] P. Phillips, Mottness, Ann. Phys. (N.Y.) **321**, 1634 (2006), July 2006 Special Issue.

[43] See Supplemental Material at http://link.aps.org/supplemental/10.1103/PhysRevB.95.035113 for an extensive comparison between IPT and the CT-QMC.

[44] O. Parcollet, G. Biroli, and G. Kotliar, Cluster Dynamical Mean Field Analysis of the Mott Transition, Phys. Rev. Lett. **92**, 226402 (2004).

[45] H. Park, K. Haule, and G. Kotliar, Cluster Dynamical Mean Field Theory of the Mott Transition, Phys. Rev. Lett. **101**, 186403 (2008).

[46] M. Balzer, B. Kyung, D. Sénéchal, A.-M. S. Tremblay, and M. Potthoff, First-order Mott transition at zero temperature in two dimensions: Variational plaquette study, Europhys. Lett. **85**, 17002 (2009).

[47] T. C. Koethe, Z. Hu, M. W. Haverkort, C. Schüßler-Langeheine, F. Venturini, N. B. Brookes, O. Tjernberg, W. Reichelt, H. H. Hsieh, H. J. Lin, C. T. Chen, and L. H. Tjeng, Transfer of Spectral Weight and Symmetry Across the Metal-Insulator Transition in VO_2, Phys. Rev. Lett. **97**, 116402 (2006).